

Unsteady convection with chemical reaction and radiative heat transfer past a flat porous plate moving through a binary mixture

Afrika Matematika

ISSN 1012-9405

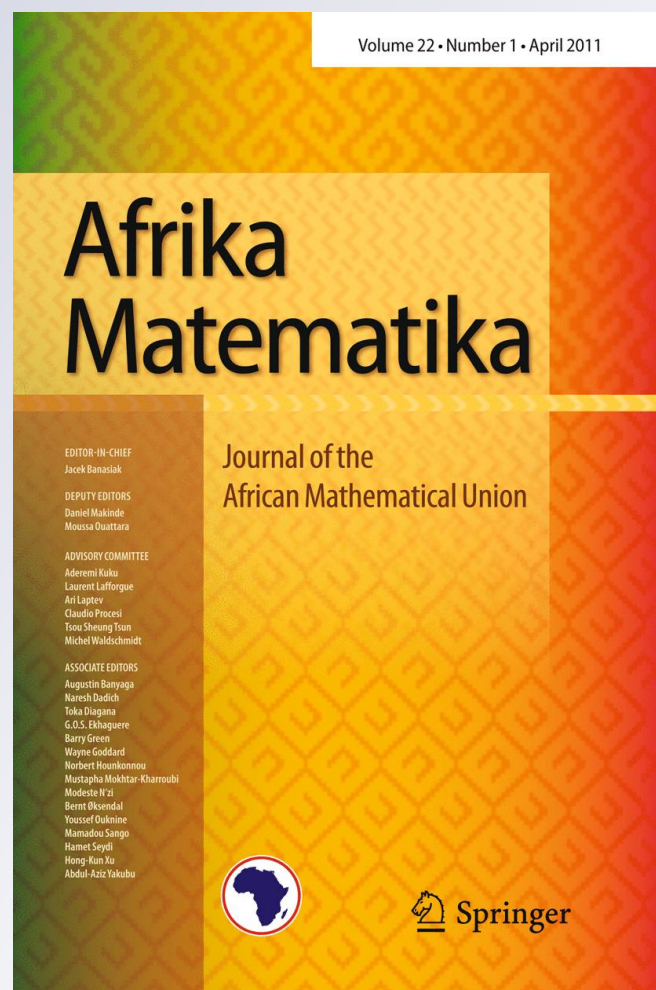
Volume 22

Number 1

Afr. Mat. (2011) 22:65-78

DOI 10.1007/s13370-011-0008-

Z



Your article is protected by copyright and all rights are held exclusively by African Mathematical Union and Springer-Verlag. This e-offprint is for personal use only and shall not be self-archived in electronic repositories. If you wish to self-archive your work, please use the accepted author's version for posting to your own website or your institution's repository. You may further deposit the accepted author's version on a funder's repository at a funder's request, provided it is not made publicly available until 12 months after publication.

Unsteady convection with chemical reaction and radiative heat transfer past a flat porous plate moving through a binary mixture

O. D. Makinde · P. O. Olanrewaju · W. M. Charles

Received: 26 April 2010 / Accepted: 20 October 2010 / Published online: 15 February 2011
© African Mathematical Union and Springer-Verlag 2011

Abstract In this paper, the problem of unsteady convection with chemical reaction and radiative heat transfer past a flat porous plate moving through a binary mixture in an optically thin environment is presented. The dimensionless governing equations for this investigation are solved numerically by the fourth-order Runge–Kutta integration scheme along with shooting technique. Numerical data for the local skin-friction coefficient, the local Nusselt number and the local Sherwood number have been tabulated for various values of parametric conditions. Graphical results for velocity, temperature and concentration profiles based on the numerical solutions are presented and discussed.

Keywords Boundary layer flow · Radiative heat transfer · Binary mixture · Arrhenius kinetics · Porous plate

Mathematics Subject Classification (2000) 80A20 · 76D10 · 65L06

List of Symbols

(x, y) Cartesian coordinates
 C_∞ Free stream concentration

O. D. Makinde (✉)
Faculty of Engineering, Cape Peninsula University of Technology, P.O. Box 1906,
Bellville 7535, South Africa
e-mail: dmakinde@yahoo.com

P. O. Olanrewaju
Department of Mathematics, Covenant University, Km. 10 Idiroko Road,
Canaanland, P.M.B. 1023, Ota, Nigeria
e-mail: oladapo-anu@yahoo.ie

W. M. Charles
Department of Mathematics, College of Natural and Applied Sciences (CoNAS),
University of Dar-es-salaam, P.O. Box 35062, Dar-es-salaam, Tanzania
e-mail: cwmahera@maths.udsm.ac.tz

(u, v)	Velocity components
C	Concentration of the fluid
T_w	Surface temperature
C_w	Surface concentration
T_∞	Free stream temperature
Da	Damköhler number
g	Gravitational acceleration
k	Thermal conductivity
Q	Heat generation coefficient
c_p	Specific heat at constant pressure
T	Fluid temperature
D	Diffusion coefficient
R_A	n th order irreversible reaction
U_0	Plate uniform velocity
R_G	Universal gas constant
Pr	Prandtl number
c	Suction parameter
E	Activation energy
S_c	Schmidt number
b	Heat generation parameter
G_r	Thermal Grashof number
G_c	Solutal Grashof number

Greek symbols

θ	Fluid temperature
φ	Fluid concentration
η	Similarity variable
γ	Activation energy parameter
β	Thermal volumetric-expansion coefficient
β_c	Concentration volumetric-expansion coefficient
σ	Stefan-Boltzmann constant
α	Absorption coefficient
ρ	Fluid density
ν	Kinematic viscosity

1 Introduction

Studies related to boundary layer flow of a binary mixture of fluids are always important in view of its applications in various branches of engineering and technology. A familiar example is an emulsion which is the dispersion of one fluid within another fluid. Typical emulsions are oil dispersed within water or water within oil. Another example where the mixture of fluids plays an important role is in multigrade oils. Polymeric type fluids are added to the base oil so as to enhance the lubrication properties of mineral oil [1]. Moreover, all industrial chemical processes are designed to transform cheaper raw materials to high value products through chemical reaction. A reactor in which such chemical transformations occur brings reactants into intimate contact by providing appropriate temperature and concentration fields for the duration of the process. Fluid dynamics plays a pivotal role in

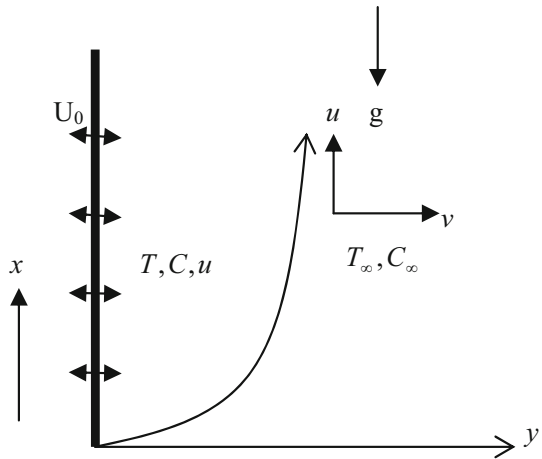
establishing relationship between the reactor hardware and reactor performance. The thermomechanical balance equations for a mixture of general materials were first formulated by Truesdell [2]. Thereafter several authors have obtained some exact solutions for the boundary layer flow of a binary mixture of incompressible Newtonian fluids [3–5]. Several problems relating to the mechanics of oil and water emulsions, particularly with regard to applications in lubrication practice, have been considered within the context of the binary mixture theory by Al-Sharif et al. [6] and Wang et al. [7]. Meanwhile, analyses of the transport processes and their interaction with chemical reactions and thermal radiation are quite difficult and are intimately connected to the underlying fluid dynamics. Such a combined analysis of chemical and physical processes constitutes the core of chemical reaction engineering. Moreover, the study of heat generation or absorption effects in moving fluids is important in view of several physical problems, such as fluid undergoing exothermic or endothermic chemical reaction. The recent advances in understanding physics of flows and computational flow modeling can make tremendous contributions in engineering and industrial processes. Sparrow and Cess [8] studied the problem of absorbing–emitting gray fluid with a black vertical plate. Using perturbation technique, they obtained solution that was applicable for small values of the conduction–radiation interaction parameter. Abdus Sattar and Hamid Kalim [9] investigated the unsteady free convection interaction with thermal radiation in a boundary layer flow past a vertical porous plate. They found that an increase in Prandtl number might lead to a reduction in the thermal boundary layer thickness. Makinde [10] studied the transient free convection interaction with thermal radiation of an absorbing–emitting fluid along a moving vertical permeable plate. The problem of unsteady hydromagnetic convection through a porous medium with combined heat and mass transfer with heat source/sink was investigated by Kamel [11]. Kandasamy et al. [12] studied the combined effects of chemical reaction, heat and mass transfer along a wedge with heat source and concentration in the presence of suction or injection. Their result shows that the flow field is influenced appreciably by chemical reaction, heat source and suction or injection at the wall of the wedge. Several recent studies on boundary layer flow coupled with heat and mass transfer can also be found in the literature [12–17].

Since no attempt has been made to analyze the nonlinear unsteady convection with n th order Arrhenius kinetics and thermal radiation over a moving vertical plate through a binary mixture with suction or injection at the plate surface in the presence of heat source, we have investigated it in this article. The similarity transformation has been utilized to convert the governing partial differential equations into ordinary differential equations and then the numerical solution of the problem is drawn using the fourth-order Runge–Kutta integration scheme along with shooting method. The analysis of the results obtained shows that the flow field is influenced appreciably by the presence of chemical reaction, heat source, buoyancy forces, thermal radiation, suction or injection at the plate surface. It is hoped that the results obtained will not only provide useful information for applications, but also serve as a complement to the previous studies.

2 Mathematical model

Consider the unsteady one-dimensional convective flow with chemical reaction and radiative heat transfer past a vertical porous plate moving through a binary mixture (Fig. 1). The fluid is assumed to be optically thin with absorption coefficient ($\alpha \ll 1$). Following Cheng [18], the approximate form of the radiative heat flux equation $\frac{\partial \bar{q}_r}{\partial y}$ is taken as the fourth power of temperature in the energy balance equation.

Fig. 1 Flow configuration and coordinate system



We choose Cartesian axes (x, y) parallel and perpendicular to the plate with velocity components are (u, v) , respectively. The flow is assumed to be in the x -direction, which is taken along the vertical plate. Under these conditions the momentum, energy and chemical species concentration balance equations governing the problem in may be written as [9–12],

$$\frac{\partial v}{\partial y} = 0 \tag{1}$$

$$\frac{\partial u}{\partial t} + v \frac{\partial u}{\partial y} = \nu \frac{\partial^2 u}{\partial y^2} + g\beta(T - T_\infty) + g\beta_c(C - C_\infty) \tag{2}$$

$$\rho c_p \left(\frac{\partial T}{\partial t} + v \frac{\partial T}{\partial y} \right) = k \frac{\partial^2 T}{\partial y^2} + Q - 4\sigma\alpha^2 T^4 \tag{3}$$

$$\frac{\partial C}{\partial t} + v \frac{\partial C}{\partial y} = D \frac{\partial^2 C}{\partial y^2} - R_A \tag{4}$$

where u and v are velocity components in x and y directions respectively, T is the temperature, t is the time, g is the acceleration due to gravity, β is the thermal expansion coefficient, β_c is the concentration expansion coefficient, ν is the kinematic viscosity, D is the chemical molecular diffusivity, k is the thermal conductivity, ρ is the density, T_w is the wall temperature, T is the free stream temperature, C_w is the species concentration at the plate surface, C_∞ is the free stream concentration, $Q = (-\Delta H)R_A$ is the heat of chemical reaction and is the activation enthalpy. We employed Arrhenius type of the n th order irreversible reaction given by,

$$R_A = k_r e^{-E/R_G T} C^n \tag{5}$$

where k_r is the chemical reaction rate, R_G is the universal gas constant and E is the activation energy parameter. The appropriate initial and boundary conditions are

$$u(y, 0) = 0, \quad T(y, 0) = T_w, \quad C(y, 0) = C_w \tag{6}$$

$$u(0, t) = U_0, \quad T(0, t) = T_w, \quad C(0, t) = C_w, \quad t > 0 \tag{7}$$

$$u \rightarrow 0, \quad T \rightarrow T_\infty, \quad C \rightarrow C_\infty \quad \text{as } y \rightarrow \infty, \quad t > 0 \tag{8}$$

where U_0 is the plate characteristic velocity. We introduce the following dimensionless quantities and parameters,

$$\begin{aligned}
 u &= U_0 F(\eta), \quad (\theta, \theta_w) = \frac{(T, T_w)}{T_\infty}, \quad (\varphi, \varphi_w) = \frac{(C, C_w)}{C_\infty}, \quad G_r = \frac{4\mathcal{V}t g \beta T_\infty}{U_0} \\
 G_r &= \frac{4\mathcal{V}t g \beta_c C_\infty}{U_0}, \quad Pr = \frac{\mathcal{V}}{\lambda}, \quad \lambda = \frac{k}{\rho c_p}, \quad Sc = \frac{\mathcal{V}}{D}, \quad \gamma = \frac{E}{R_G T_\infty}, \quad \eta = \frac{y}{2\sqrt{\mathcal{V}t}} \quad (9) \\
 k_0 &= k_r e^{\frac{-E}{R_G T_\infty}}, \quad b = \frac{(-\Delta H)C_\infty}{\rho c_p T_\infty}, \quad Ra = \frac{16\sigma \alpha^2 t T_\infty^3}{\rho c_p}, \quad Da = 4tk_0 C_\infty^{n-1}
 \end{aligned}$$

From Eq. (1), v is either constant or a function of time. Following Makinde [10], we choose

$$v = -c \left(\frac{\mathcal{V}}{t} \right)^{\frac{1}{2}} \quad (10)$$

where $c > 0$ is the suction parameter and $c < 0$ is the injection parameter. Equations (2)–(4) then become,

$$F'' + 2(\eta + c)F' = -G_r(\theta - 1) - G_c(\varphi - 1) \quad (11)$$

$$\frac{1}{Pr} \theta'' + 2(\eta + c)\theta' = -bDa\varphi^n \exp\left(\gamma \left(1 - \frac{1}{\theta}\right)\right) + Ra\theta^4 \quad (12)$$

$$\frac{1}{Sc} \varphi'' + 2(\eta + c)\varphi' = Da\varphi^n \exp\left(\gamma \left(1 - \frac{1}{\theta}\right)\right) \quad (13)$$

with the boundary conditions

$$F(0) = 1, \quad \theta(0) = \theta_w, \quad \varphi(0) = \varphi_w, \quad F(\infty) = 0, \quad \theta(\infty) = 1, \quad \varphi(\infty) = 1 \quad (14)$$

where prime symbol represents derivatives with respect to η , b is the heat generation parameter, Da is the Damköhler number, Ra is the radiation parameter, γ is the activation energy parameter, G_r is the thermal Grashof number and G_c solutal Grashof number. Other physical quantities of interest in this problem, namely; the skin friction parameter (τ) and the Nusselt number (Nu) and Sherwood number (Sh) can be easily computed. These quantities are defined in dimensionless terms as: $\tau = -F'(0)$, $Nu = \theta'(0)$, and $Sh = \varphi'(0)$.

3 Numerical procedure

The set of non-linear ordinary differential equations (11)–(13) with boundary conditions in (14) have been solved numerically by using the Runge–Kutta integration scheme with a modified version of the Newton–Raphson shooting method with $G_c, G_r, \gamma, Ra, Da, \theta_w, \varphi_w, c, b, n, Sc,$ and Pr as prescribed parameters. The computations were done by a program which uses a symbolic and computational computer language MAPLE [19]. A step size of $\Delta\eta = 0.001$ was selected to be satisfactory for a convergence criterion of 10^{-7} in nearly all cases. The value of y_∞ was found to each iteration loop by the assignment statement $\eta_\infty = \eta_\infty + \Delta\eta$. The maximum value of η_∞ , to each group of parameters $G_c, G_r, \gamma, Ra, Da, \theta_w, \varphi_w, c, b, n, Sc,$ and Pr is determined when the values of unknown boundary conditions at $\eta = 0$ not change to successful loop with error less than 10^{-7} .

Table 1 Computations showing values of $\varphi'(0)$, $F'(0)$ and $\theta'(0)$ for $b = 1$, $\gamma = \theta_w = 0.1$.

Da	Sc	c	Ra	n	G_r	G_c	$\varphi'(0)$	$F'(0)$	$\theta'(0)$
0.1	0.22	0.1	0.1	1	0.1	0.1	0.45299820	-1.363220887	0.940099503
0.2	0.22	0.1	0.1	1	0.1	0.1	0.40825426	-1.362524805	1.017519463
0.3	0.22	0.1	0.1	1	0.1	0.1	0.36731514	-1.362049836	1.085715626
0.1	0.62	0.1	0.1	1	0.1	0.1	0.76629786	-1.347622867	0.950736367
0.1	0.78	0.1	0.1	1	0.1	0.1	0.86343256	-1.344659445	0.952741674
0.1	0.22	1.0	0.1	1	0.1	0.1	0.68928294	-2.737972223	1.796428656
0.1	0.22	-0.1	0.1	1	0.1	0.1	0.40619537	-1.108018112	0.779055070
0.1	0.22	-1.0	0.1	1	0.1	0.1	0.22690545	-0.311091119	0.244583695
0.1	0.22	0.1	0.2	1	0.1	0.1	0.45322418	-1.370176013	0.867590872
0.1	0.22	0.1	0.3	1	0.1	0.1	0.45342377	-1.375748994	0.812511169
0.1	0.22	0.1	0.1	3	0.1	0.1	0.46481660	-1.363537283	0.914076370
0.1	0.22	0.1	0.1	5	0.1	0.1	0.46999599	-1.363673665	0.903949316
0.1	0.22	0.1	0.1	1	1.0	0.1	0.45299820	-1.716737895	0.940099503
0.1	0.22	0.1	0.1	1	5.0	0.1	0.45299820	-3.287924599	0.940099503
0.1	0.22	0.1	0.1	1	0.1	1.0	0.45299820	-1.950303852	0.940099503
0.1	0.22	0.1	0.1	1	0.1	5.0	0.45299820	-4.559561477	0.940099503

4 Results and discussion

In order to get a clear insight of the physical problem, the velocity, temperature and concentration have been discussed by assigning numerical values to the parameters encountered in the problem. To be realistic, the values of Schmidt number (Sc) are chosen for hydrogen ($Sc = 0.22$), water vapour ($Sc = 0.62$), ammonia ($Sc = 0.78$) and Propyl Benzene ($Sc = 2.62$) at temperature 25°C and one atmospheric pressure. The values of Prandtl number is chosen to be $Pr = 0.71$ which represents air at temperature 25°C and one atmospheric pressure. Attention is focused on positive values of the buoyancy parameters i.e. Grashof number $G_r > 0$ (which corresponds to the cooling problem) and solutal Grashof number $G_c > 0$ (which indicates that the chemical species concentration in the free stream region is less than the concentration at the boundary surface). The cooling problem is often encountered in engineering applications; for example in the cooling of electronic components and nuclear reactors. It should be mentioned here that $Da > 0$ indicates an increase in the chemical reaction rate. From Table 1, it is noteworthy that the heat transfer rate increases while both mass transfer rate and skin friction decreases with increasing rate of chemical reaction. It is seen that the effect of increasing values of Sc , $c > 0$, Ra , n , G_r and G_c is to increase the mass transfer rate and the skin friction at the moving plate surface. Further, it is found that the heat transfer rate at the plate surface increases with increasing values of Da , Sc , $c > 0$ and decreases with increasing values of Ra , n .

4.1 Velocity profiles

In Figs. 2, 3 and 4, we presented the behaviour of the fluid velocity for various material parameters. Figures 2 and 3 illustrate the effect of the buoyancy forces (G_r and G_c) on the horizontal velocity in the momentum boundary layer. The fluid velocity is highest at the moving plate surface and decreases to the free stream zero value far away from the plate satisfying the boundary condition. As the parameter values of G_r and G_c increase in the presence of uniform suction at the plate surface, the flow rate retard and thereby giving rise to a decrease in the velocity profiles. The momentum boundary layer thickness generally

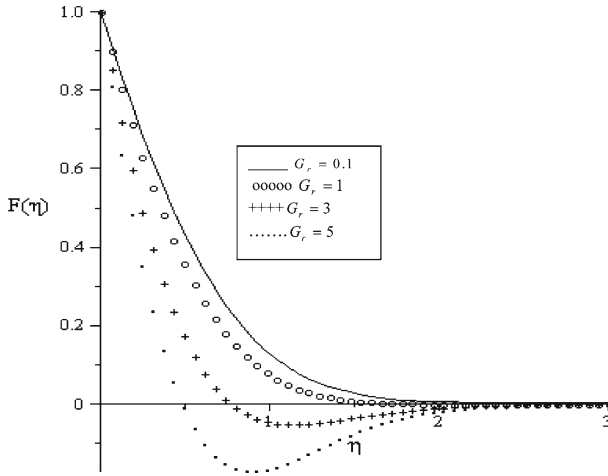


Fig. 2 Variation of the boundary layer velocity profiles with increasing values of thermal Grashof number when $G_c = \gamma = Ra = Da = \theta_w = \varphi_w = c = 0.1$, $b = n = 1$, $Sc = 0.62$

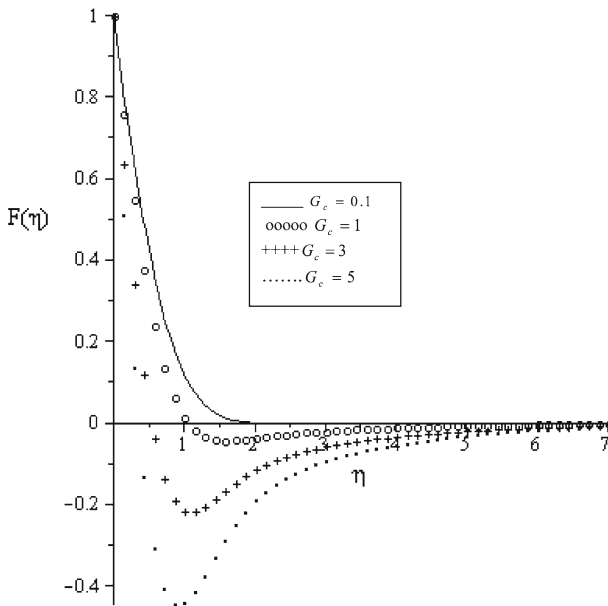


Fig. 3 Variation of the boundary layer velocity profiles with increasing values of the solutal Grashof number when $G_r = \gamma = Ra = Da = \theta_w = \varphi_w = c = 0.1$, $b = n = 1$, $Sc = 0.62$

decreases with increasing values of G_r and G_c . Meanwhile, it is interesting to note that a reverse flow occurs within the boundary layer as the intensity of buoyancy forces increases. Figure 4 illustrates the effect of wall suction and injection on the horizontal velocity in the momentum boundary layer. The trend of the velocity profiles in this figure is same as those shown in Fig. 2. It is observed that the momentum boundary layer thickness decreases with increasing wall suction ($c > 0$) and increases with increasing wall injection ($c < 0$).

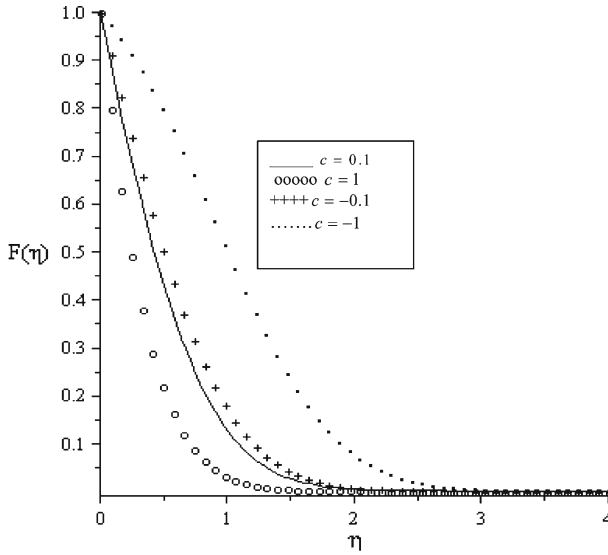


Fig. 4 Variation of the boundary layer velocity profiles with increasing values of suction/injection parameter when $G_c = \gamma = Ra = Da = \theta_w = \varphi_w = c = 0.1$, $b = n = 1$, $Sc = 0.62$

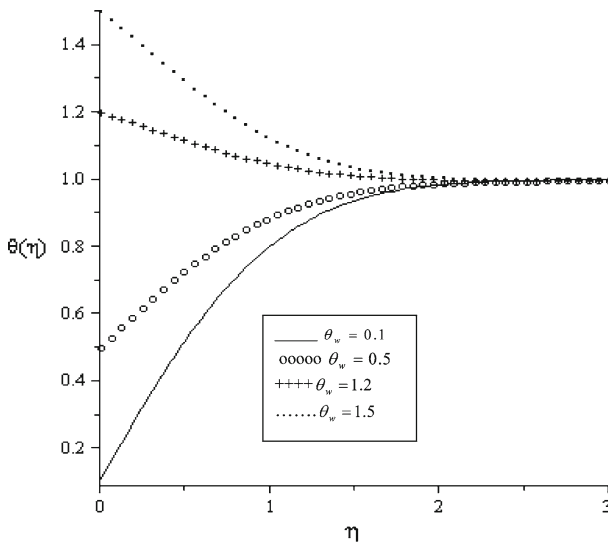


Fig. 5 Variation of the boundary layer temperature profiles with increasing values of the wall temperature parameter when $G_c = G_r = \gamma = Ra = Da = \theta_w = \varphi_w = c = 0.1$, $b = n = 1$, $Sc = 0.62$

4.2 Temperature profiles

The effects of various material parameters on the fluid temperature are illustrated in Figs. 5, 6, 7, 8 and 9. Figure 5 depicts the variation of temperature profile against spanwise coordinate η for varying values of wall temperature parameter and fixed values of other physical parameter in the presence of uniform suction. It is interesting to note from this figure that the fluid

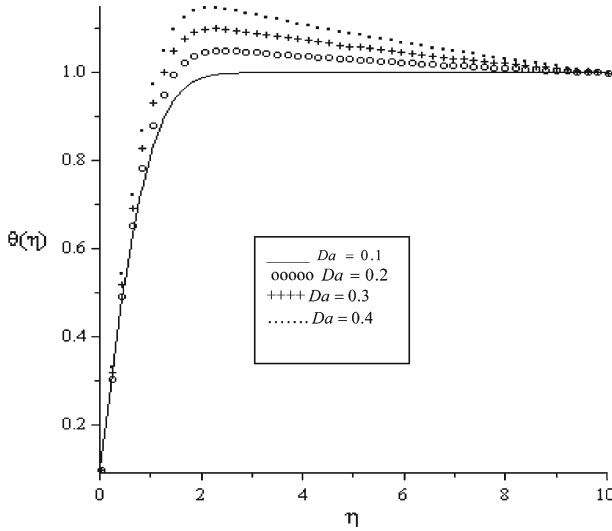


Fig. 6 Variation of the boundary layer temperature profiles with increasing values of the Damköhler number when $G_r = G_c = \gamma = Ra = Da = \varphi_w = c = 0.1$, $b = n = 1$, $Sc = 0.62$

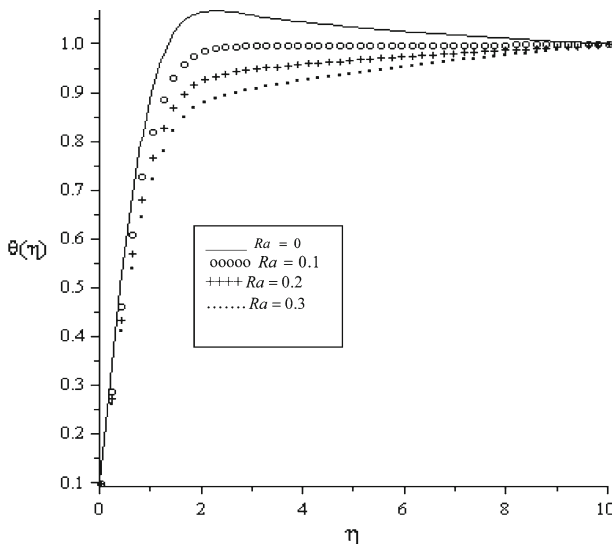


Fig. 7 Variation of the boundary layer temperature profiles with increasing values of the radiation parameter when $G_r = G_c = \gamma = Da = \theta_w = \varphi_w = c = 0.1$, $b = n = 1$, $Sc = 0.62$

temperature increases (or decreases) toward the free stream temperature whenever the plate temperature is lower (or higher) than the free stream temperature. Figure 6 shows the effects of exothermic chemical reaction rate on the fluid temperature profile within the boundary layer when the wall temperature is lower than the free stream temperature in the presence of uniform suction. An increase in the fluid temperature is observed with increasing value of Da . This can be attributed to internal heat generation in the fluid due to Arrhenius kinetics.

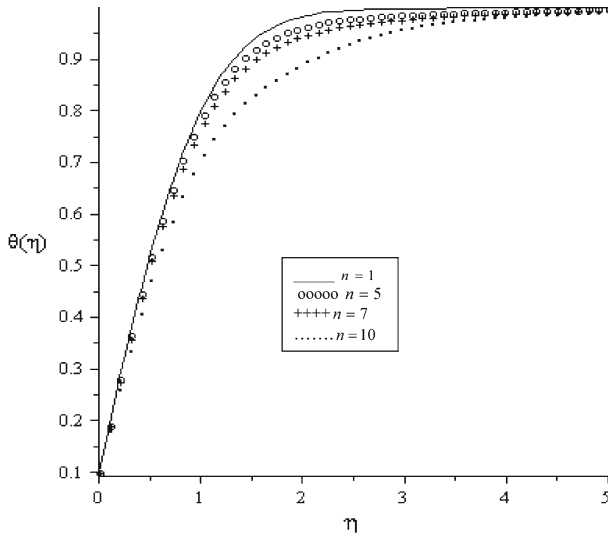


Fig. 8 Variation of the boundary layer temperature profiles with increasing values of the reaction order index when $G_r = G_c = Ra = \gamma = Da = \theta_w = \varphi_w = c = 0.1$, $b = 1$, $Sc = 0.62$

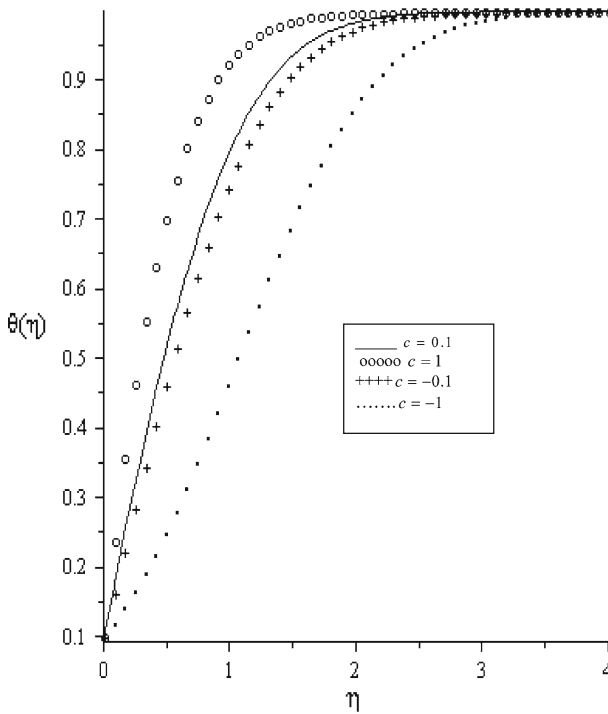


Fig. 9 Variation of the boundary layer temperature profiles with increasing values of suction/injection parameter when $G_c = G_r = \gamma = Ra = Da = \theta_w = \varphi_w = c = 0.1$, $b = n = 1$, $Sc = 0.62$

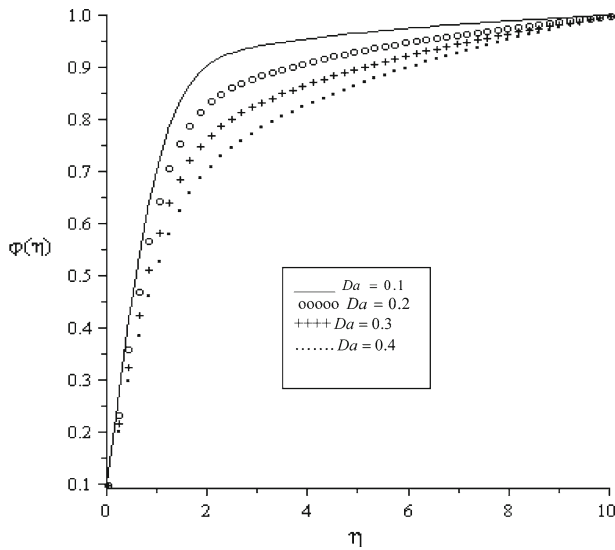


Fig. 10 Variation of the boundary layer concentration profiles with increasing values of the Damköhler number when $G_r = G_c = \gamma = Ra = \theta_w = \phi_w = c = 0.1$, $b = n = 1$, $Sc = 0.62$

Figure 7 represents graph of temperature distribution with spanwise coordinate η for different values of radiation parameter Ra . From this figure, it is seen that the fluid temperature starts from a minimum value at the moving plate surface and increases till it reaches the free stream temperature value at the end of the boundary layer for all the values of radiation parameter. The effect of increasing value of radiation absorption parameter is to decrease the fluid temperature within the boundary layer. Figure 8 represents the temperature profiles for different values of reaction order parameter (n). It is observed that the fluid temperature decreases with increasing order of Arrhenius chemical reaction. The effect of suction/injection parameter on the fluid temperature is highlighted in Fig. 9. The trend of the temperature profiles in this figure is same as those shown in Fig. 8. It is observed that the fluid temperature increases with suction and decreases with injection.

4.3 Concentration profiles

Figures 10, 12 and 13 depict chemical species concentration profiles against spanwise coordinate η for varying values of thermophysical parameters in the boundary layer. Generally, whenever the species concentration at the plate surface is lower than the free stream concentration, a gradual increase in concentration profile towards the free stream value is observed. The trend is reversed whenever the species concentration at the plate surface is higher than that of the free stream. The effect of chemical reaction rate parameter Da as shown in Fig. 10 is very important in concentration field. Chemical reaction increases the rate of interfacial mass transfer. The reaction reduces the local concentration, thus increasing its concentration gradient and its flux. As seen from the graph, an increase in Da causes a decrease in the concentration of the chemical species in the boundary layer. Figure 11 depicts the effect of Schmidt number (Sc) on concentration profiles. We observed from this figure that chemical species concentration within the boundary layer increases with an increase in Sc . Physically, an increase in the Schmidt number means a decrease in molecular diffusivity (D) of the

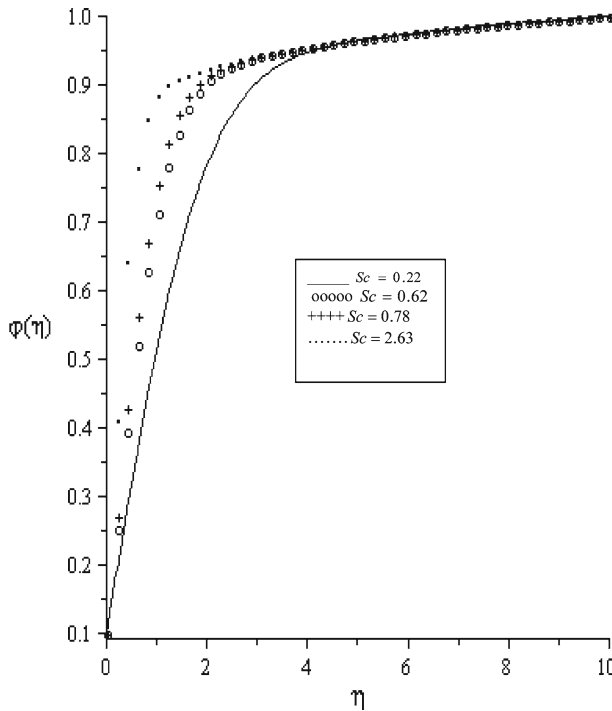


Fig. 11 Variation of the boundary layer concentration profiles with increasing values of the Schmidt number when $G_r = G_c = Ra = \gamma = Da = \theta_w = \varphi_w = c = 0.1$, $b = n = 1$

chemical species. Hence, the concentration of the species is higher for higher values of Sc and lower for small values of Sc . Similar trend is observed with increasing value of reaction order parameter (n) as shown in Fig. 12. The effect of suction/injection parameter on the chemical species concentration in the boundary layer is depicted in Fig. 13. From this figure, it is seen that the species concentration within the boundary layer is higher for suction and lower for injection.

5 Conclusions

The effects of n th order Arrhenius chemical reaction, thermal radiation, suction/injection and buoyancy forces on unsteady convection of a viscous incompressible fluid past a vertical porous plate is studied. A set of non-linear coupled differential equations governing the fluid velocity, temperature and chemical species concentration is solved numerically for various material parameters. A comprehensive set of graphical results for the velocity, temperature and concentration is presented and discussed. Our results reveal among others, that the fluid velocity within the boundary layer decreases with increasing values of buoyancy forces and wall suction, and increases with wall injection. The temperature profile decreases in the presence of radiation absorption Ra and increases with increasing rate of exothermic chemical reaction Da and reaction order n . In addition, the chemical species concentration within the boundary layer decreases with increasing Da and wall injection.

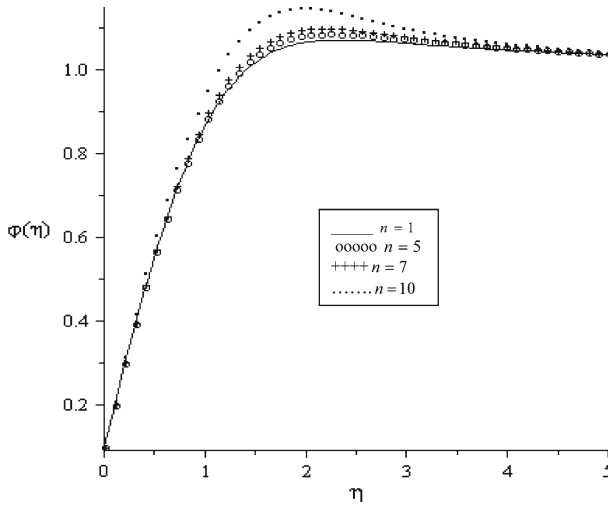


Fig. 12 Variation of the boundary layer concentration profiles with increasing values of the reaction order index when $G_r = G_c = Ra = \gamma = Da = \theta_w = \phi_w = c = 0.1$, $b = 1$, $Sc = 0.62$

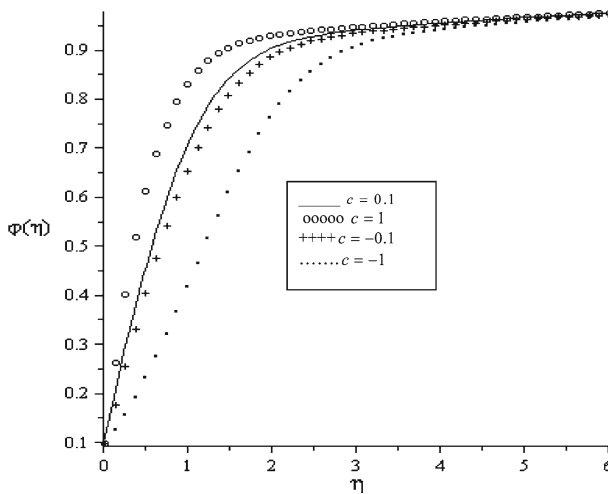


Fig. 13 Variation of the boundary layer concentration profiles with increasing values of suction/injection parameter when $G_c = G_r = \gamma = Ra = Da = \theta_w = \phi_w = 0.1$, $b = n = 1$, $Sc = 0.62$

Acknowledgments ODM would like to thank the National Research Foundation of South Africa Thuthuka programme for financial support. Dr. Olanrewaju visited CPUT on postdoctoral studies.

References

1. Dai, F., Khonsari, M.M.: A theory of hydrodynamic lubrication involving the mixture of fluids. *J. Appl. Mech.* **61**, 634–641 (1994)
2. Truesdell, C.: Sulle basi della termomeccanica. *Rend. Lince* **22**(8), 33–38, 158–166 (1957)
3. Mills, N.: Incompressible mixtures of Newtonian fluids. *Int. J. Eng. Sci.* **4**, 97–112 (1966)

4. Beevers, C.E., Craine, R.E.: On the determination of response functions for a binary mixture of incompressible Newtonian fluids. *Int. J. Eng. Sci.* **20**, 737–745 (1982)
5. Göğüş, M.: The steady flow of a binary mixture between two rotating parallel non-coaxial disks. *Int. J. Eng. Sci.* **26**, 665–677 (1992)
6. Al-Sharif, A., Chamnirasart, K., Rajagopal, K.R., Szeri, A.Z.: Lubrication with binary mixtures: liquid-liquid emulsion. *J. Tribol.* **115**, 46–55 (1993)
7. Wang, S.H., Al-Sharif, A., Rajagopal, K.R., Szeri, A.Z.: Lubrication with binary mixtures: liquid-liquid emulsion an EHL conjunction. *J. Tribol.* **115**, 515–522 (1993)
8. Sparrow, E.M., Cess, R.D.: *Radiation Heat Transfer*, Augmented edition. Hemisphere Publishing Coop., Washinton (1978)
9. Abdus Sattar, M.D., Hamid Kalim, M.D.: Unsteady free-convection interaction with thermal radiation in a boundary layer flow past a vertical porous plate. *J. Math. Phys. Sci.* **30**, 25–37 (1996)
10. Makinde, O.D.: Free convection flow with thermal radiation and mass transfer past a moving vertical porous plate. *Int. Commun. Heat Mass Transf.* **32**, 1411–1419 (2005)
11. Kamel, M.H.: Unsteady MHD convection through porous medium with combined heat and mass transfer with heat source/sink. *Energy Convers. Manag.* **42**, 393–405 (2001)
12. Kandasamy, R., Periasamy, K., Sivagnana Prabhu, K.K.: Effects of chemical reaction, heat and mass transfer along a wedge with heat source and concentration in the presence of suction or injection. *Int. J. Heat Mass Transf.* **48**, 1388–1394 (2005)
13. Makinde, O.D., Moitshek, R.J.: On non-perturbative techniques for thermal radiation effect on natural convection past a vertical plate embedded in a saturated porous medium. *Math. Probl. Eng.* **2008**, 689074 (2008)
14. Makinde, O.D.: On MHD boundary-layer flow and mass transfer past a vertical plate in a porous medium with constant heat flux. *Int. J. Num. Methods Heat Fluid Flow* **19**(3/4), 546–554 (2009)
15. Ogulu, A., Makinde, O.D.: Unsteady hydromagnetic free convection flow of a dissipative and radiating fluid past a vertical plate with constant heat flux. *Chem. Eng. Commun.* **196**(4), 454–462 (2009)
16. Makinde, O.D., Olanrewaju, P.O.: Buoyancy effects on thermal boundary layer over a vertical plate with a convective surface boundary condition. *Trans. ASME J. Fluid Eng.* **132**, 044502(1–4) (2010)
17. Sibanda, P., Makinde, O.D.: On steady MHD flow and heat transfer due to a rotating disk in a porous medium with Ohmic heating and viscous dissipation. *Int. J. Num. Methods Heat Fluid Flow* **20**(3), 269–285 (2010)
18. Cheng, P.: Two dimensional radiation gas flow by moment method. *AIAA J* **2**, 1662–1664 (1964)
19. Heck, A.: *Introduction to Maple*, 3rd edn. Springer-Verlag, New York (2003)